



## Treatment of power plant wastewater using reverse osmosis process

Hiba A. Mohammed<sup>a</sup>, Dawood E. Sachit<sup>a,\*</sup>, Mustafa H. Al-Furaiji<sup>b</sup>

<sup>a</sup>*Environmental Engineering Department, College of Engineering, Mustansiriyah University, Iraq, emails: Dawood.sachit@uomustansiriyah.edu.iq (D.E. Sachit), hiba1997ahmed@gmail.com (H.A. Mohammed)*

<sup>b</sup>*Environment and Water Directorate, Ministry of Science and Technology, Baghdad, Iraq, email: alfurajji79@gmail.com*

Received 10 June 2022; Accepted 10 December 2022

---

### ABSTRACT

Water pollution control is becoming a significant concern. Pollution may be reduced using a variety of technologies. This study aims to use a flat sheet reverse osmosis (RO) membrane with micro-filtration (MF) and ultrafiltration (UF) pretreatment to treat actual wastewater samples from the South Baghdad Power Plant-1. The SEM images of the fouled RO membranes revealed that using UF as a pretreatment process for the feedwater reduced the extent of the fouling across the surface of the RO membranes by 50%. Consequently, the initial permeate flux of the run conducted with UF was higher by about 40% than the initial permeate flux of the run conducted by using MF. In addition, when UF was used, chemical oxygen demand (COD) and total dissolved solids (TDS) removal percentages increased by 14% and 6%, respectively. Also, the removal percentages of the oil and Cr<sup>3+</sup> increased up to 99.5%. Furthermore, the SEM images showed that the backwashed membrane was nearly similar to the clean membrane in its appearance and in terms of contaminant removal. On the other hand, the initial permeate flux of the backwashing run was about 9% lower than the original permeate flux. Experiments have shown that employing a MF/UF pretreatment before the RO process is feasible. The quality of the water was enhanced by the reduction of heavy metals, oil, COD, and TDS concentrations, demonstrating the effectiveness of the used membrane technology in both wastewater treatment and the production of ultrapure water. Additionally, backwashing was effective in reactivating the RO membrane, and therefore, it can be utilized as an alternative option to chemical cleaning.

*Keywords:* Membrane; Reverse osmosis; Heavy metals; Fouling; Backwashing

---

### 1. Introduction

Water treatment technologies such as adsorption and membrane processes are utilized to remove contaminants such as salts, toxic metals, and oils from wastewater [1]. Heavy metals are a serious environmental concern that must be treated before being released into the natural environment to ensure that the discharge complies with current national environmental standards [2,3]. The effluent from power plants often contains dangerous pollutants including heavy metals, which have serious consequences for the environment. Oil is another harmful pollutant found in

wastewater [4]. Membrane technologies have drawn much interest in treating industrial wastewater [2]. Membranes are used to treat water for a wide range of purposes, including softening, desalination, and removing specific contaminants, such as metals and solids [3].

Among the technologies employed in water reclamation, reverse osmosis (RO) has been found to be one of the most advanced separation technology for water reuse in power plant applications [5,6]. The RO technology is widely utilized owing to its straightforward design, high production capacity, excellent power effectiveness, and significantly lower initial and maintenance expenses [7]. RO is a

---

\* Corresponding author.

pressure-driven technology utilized to remove dissolved salt and metal ions from wastewater due to its characteristic porous structure and high separation efficiency [3]. The difference in pressure among between the feedwater and the interior membrane forces solute particles that are smaller than the membrane pore through the membrane as permeate. In contrast, particles that are larger than the membrane pore are concentrated and captured as retentate [6]. Semi-permeable RO membranes are made of polymeric materials such as cellulose acetate (CA), polyamide (PA), thin-film composite polyamide (TFC-PA) and other polymers [8]. The TFC-PA is the most advanced RO membrane commercially available [9].

The successful utilization of the RO process for wastewater treatment comes with several problems, such as concentration polarization, fouling, high capital and operating costs, and the problem of concentrate disposal [10]. However, fouling remains key problem for RO applications [11]. The predominant contributors to membrane fouling are the deposition of metals, salts, organic matter, and, in specific circumstances, suspended solids on the top of the membrane [6]. Fouling types that are characterized based on the properties of the foulants present in the feedwater can include biological fouling, colloidal fouling, scaling fouling, and organic fouling [12,13].

Control of fouling is essential in designing and operating membrane processes [14]. Many efforts have been made to reduce fouling since it causes a decline in permeate flux, a rise in operating pressure, a loss of treated water quality, and a deterioration of the RO membrane [15]. The application of pretreatment to RO systems is studied to increase feedwater quality and ensure the improvement of RO water treatment performance and increase membrane life [6,15,16]. Membrane technology, specifically ultrafiltration (UF)/MF, is becoming a popular pretreatment option for controlling RO membrane fouling because it can achieve excellent efficiency in removing suspended matter, colloids, and microorganisms. The treatment can also deliver excellent pollutant removal and minimize turbidity [17]. It is recommended that chemical cleaning be minimized or avoided in large-scale RO membrane systems because frequent chemical cleaning will shorten membrane life and raise operating and maintenance expenses owing to residual chemical disposal. In contrast, efficient physical cleaning methods can lessen the need for chemical cleaning, extending the membrane's useful life. Performing a regular backwashing process is an integral part of physical cleaning that ensures the membrane system lasts as long as possible and continues to perform well. Consequently, this technique is essential to sustaining high levels of safety, quality, and dependability in water delivery. Therefore, backwashing can be an alternative option to reduce membrane fouling [14,18].

Fouling of RO membranes has received considerable attention in recent years. The most effective approach for determining the causes of membrane fouling is by performing a membrane autopsy [13]. The aim of the autopsy is to discover why a blockage happened and how to avoid it in the future, as well as to determine the best options for cleaning conditions and membrane reactivation [2]. Several studies on fouled membrane autopsy have been published to assess the morphology and degree of fouling. For example,

Sachit and Veenstra [19] studied the precipitated pollutants on the membrane surface from various feedwaters using SEM, EDXS, and FTIR testing. They also used a 0.1- $\mu\text{m}$  MF as a pretreatment for the feedwater. They found that the fouling was mostly organic, and the main deposit was calcium carbonate ( $\text{CaCO}_3$ ). In another research, Koyuncu and Wiesner [20] used SEM and EDXS analysis to study the morphology of the foulant materials and their compositions. They reported that the predominant salts precipitated on the RO membrane were calcium carbonate ( $\text{CaCO}_3$ ) and calcium sulfate ( $\text{CaSO}_4$ ). Additionally, their research revealed that changes in organic matter content might alter the crystal shape of calcium carbonate, increasing its precipitation on a reverse osmosis membrane. In a different study, Jendoubi et al. [21] investigated the performance of membrane autopsy of RO membrane deposits from industrial wastewater using X-ray and IR spectra. The autopsy results showed that the fouling is primarily caused by suspended particles and microorganism development, which were not captured by the various pretreatment filtrations.

This paper investigates the performance of the RO process in removing heavy metals and organic matter with the use of MF and UF as pretreatment methods for the feedwater. Furthermore, it examines the influence of backwashing on the RO membrane reactivation using SEM, AFM, and FTIR tests.

## 2. Materials and methods

### 2.1. Materials

The membrane used in this research was TFC-PA RO membrane Model Bw30-4040 (DOW Film-Tec Corporation, USA). For MF, a 5 and 1- $\mu\text{m}$  filter cartridge (PP filter, Authentic American Life, Vietnam) were used. A 0.01- $\mu\text{m}$  ultrafilter (UF) membrane (Sterlitech Corporation, Kent, WA, USA) was also employed. The effluent utilized in this study was taken at the discharge point of the treatment plant of South Baghdad Gas Power Plant-1 in Baghdad, Iraq. Table 1 shows the water quality analysis of the power

Table 1  
Water quality analysis of the power plant wastewater sample before treatment and NEQS [22]

Parameter	Value	NEQS
pH	8.5	6–10
Temperature	19°C	40°C
TDS	763 mg/L	350 mg/L
COD	136 mg/L	150 mg/L
Oil	18.4 mg/L	10 mg/L
Zn <sup>2+</sup>	0.96 mg/L	1 mg/L
Cu <sup>2+</sup>	0.85 mg/L	1 mg/L
Cr <sup>3+</sup>	1.95 mg/L	1 mg/L
Fe <sup>3+</sup>	1.02 mg/L	1 mg/L
Cl <sup>-</sup>	80 mg/L	1 mg/L
NO <sup>-</sup>	29.1	–
SO <sub>4</sub> <sup>2-</sup>	300	600
PO <sub>4</sub> <sup>3-</sup>	3.2	–

plant wastewater sample and the acceptable range of values according to the current National Environmental Quality Standards (NEQS) [22].

## 2.2. Characterization methods

The surface and cross-sectional structures of the RO membrane were examined using a scanning electron microscope (SEM) image (EM10C, ZEISS, Germany). Atomic force microscopy (AFM) (Angstrom Advanced Inc., U.S.A) was used to measure the average diameter and the roughness of the membrane surface. To determine the effective groups of organic materials precipitated on RO membrane surfaces, the Fourier transform infrared spectroscopy (FTIR) (Spectrum 2, Perkin Elmer, USA) spectrum was conducted. Additionally, membrane samples were carefully sliced and preserved in sealed plastic containers to prevent morphological changes in the foulants deposited on the RO membrane surface. Moreover, the concentration of heavy metals in the permeate water was measured using the atomic absorption spectrophotometer (Shimadzu, AA-6800), and the concentration of oil was measured using an oil content analyzer (Horiba, OCMA-350). An ultraviolet-visible spectrum (UV-vis) spectrophotometer (DR-3600, Germany) was used to determine the chemical oxygen demand (COD) concentration in a power plant wastewater sample. Furthermore, a laboratory multi-meter (HQ430d, Flexi, Hach Company) was used to measure the total dissolved solids (TDS) concentration. In addition, gas chromatography-mass spectrometry (GC-MS) (Agilent, USA) was used to identify different contaminants within the power plant's wastewater sample.

## 2.3. RO performance test

Experiments were carried out in a SEPA CF Membrane Element Cell with a cross-flow filtration unit (Sterlitech Corporation, USA). The Membrane Element Cell can accommodate a flat sheet membrane with dimensions approximately equal to 19 cm × 14 cm and can withstand pressure up to 6,895 kPa (1,000 psi). A magnetic stirrer (ISOLAB, Laborgerate GmbH) was utilized to stir the power plant real wastewater at a moderate speed to ensure solution homogeneity. To study the impact of pretreatment on the membrane fouling, a low-pressure feeding pump (AP-100 Booster pump, Aqua Pura Instrument Co., China) was used to pump a 4-L batch of wastewater from the wastewater tank to the feed tank at a 2.5 L/min constant flow rate through 5 and 1 μm filter cartridges to keep big particles from damaging the membrane. Then, the feedwater was delivered to the break tank via an UF membrane. The feedwater was filtered across the UF membrane under the same experimental conditions as the RO membrane run, excluding the feed pressure set at 150 psi (10 bar). Finally, a high-pressure pump (M-03S Hydracell CC Pump, Wanner Engineering, USA) was used to pump the feedwater through the RO membrane filtration cell at the same flow rate. Using two high-pressure needle valves (SS-1RS6, Swagelok, CA), the system pressure was kept at 300 psi (20 bar). Fig. 1a illustrates a sketch of the RO membrane unit used in the experiment. Additionally,

to evaluate the impact of backwashing on the membrane efficiency and fouling formation, the membrane was inverted to the other side (the fouling became on the permeate side) and placed inside the SEPA CF Membrane Element Cell (Fig. 1b). Then, a 4-L of deionized water (DI) was pumped through the membrane from the feed side to the permeate side under similar circumstances as the RO membrane run, except for the feed pressure, which was maintained at 75 psi (5 bar) for about 10 min. More information about experimental system setup can be found elsewhere [23].

The duration of each experiment was 3 h, and the permeate flux was measured every 30 min. The TDS of the permeate and concentrate were also determined using a laboratory multi-meter (HQ430d, Flexi, Hach company). An oil content analyzer (Horiba, OCMA-350) was used to measure the accurate oil concentration in the permeate. Using the highly stable S-316 chlorofluorocarbon extracting solvent (Horiba, USA), oil is extracted from the permeate sample and placed into the attached cell and set to the device. The measurement of the device takes 30–60 s using the non-dispersive infrared spectroscopy (NDIR) method. Then, the result of the analysis is displayed in mg/L. At the end of each experiment, a sample of RO membrane was obtained for examination utilizing SEM, AFM, and FTIR tests.

The permeate water volume passing across the active membrane area over time was used to compute the permeate flux, as illustrated in Eq. (1) [24]. The rejection percentage of salt ( $R$ ) was measured by using Eq. (2) [25]. Moreover, the recovery of water ( $r$ ) was determined by using Eq. (3) [12]. In addition, COD and TDS removal percentage can be found as described in Eq. (4) [4]. The calculation and assessment of the selected index are shown in Table 2.

The procedure described above was repeated for a total of 4 runs. In run 1, the 5-μm filter was used alone as a pretreatment method for the wastewater. While in run 2, the 1-μm filter was used alone as a pretreatment method for the wastewater. In run 3, the 1-μm filter was used with the UF membrane to treat the power plant wastewater before being mounted to the Membrane Element Cell. Additionally, in run 4, the 1-μm filter was used as a pretreatment, and then a backwashing process for the fouled membrane was performed. The key variables in the conducted runs were four different treatment techniques which are listed in Table 3.

## 3. Results and discussion

### 3.1. Wastewater analysis

#### 3.1.1. COD and TDS test results

Table 4 summarizes the experimental results, including COD and TDS concentrations of feedwater in each run. According to the findings, the lowest levels of COD and TDS in the treated wastewater (RO permeate) were in run 3, where Mf and UF were both used as pretreatments of the wastewater before it was introduced into the RO system. During this run, the concentration of COD reduced from 136 to 12 mg/L, and the concentration of TDS decreased from 763 to 10.37 mg/L. On the other hand, the concentrations of COD and TDS were the highest in run 1, which utilized the 5 μm filter for the pretreatment.

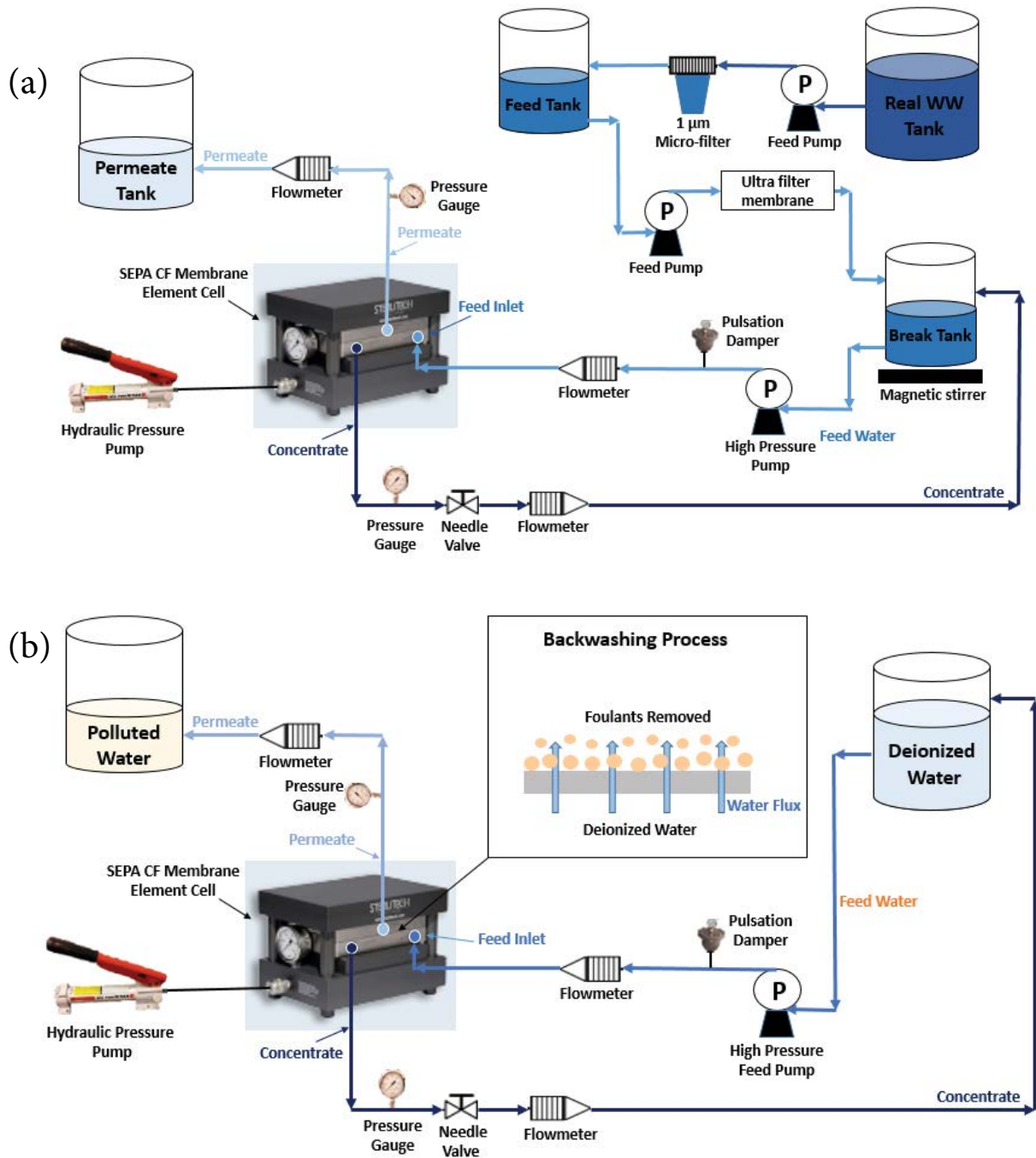


Fig. 1. (a). A sketch of the RO membrane unit used in the experiment. Adapted from [23]. (b) The experimental drawing of the backwashing process for the fouled RO membrane.

### 3.1.2. Heavy metals and oil results

The concentrations and removal percentages of heavy metals and oil from the power plant wastewater sample are shown in Table 5, along with the allowable values according to the NEQS [22]. The results showed that the concentrations of heavy metals and oil in the treated wastewater were significantly reduced below the NEQS limits by using MF/UF as a pretreatment before the RO system (run 3). The removal percentages for  $Zn^{2+}$ ,  $Cu^{2+}$ ,  $Cr^{3+}$ ,  $Fe^{3+}$ , and oil were 93.8%, 94.1%, 99.5%, 98%, and 99.5%, respectively.

### 3.1.3. GC-MS test results

GC-MS analysis of the wastewater sample was conducted to determine the percentage frequency of detection of compounds used to identify potential sources of contamination in wastewater. The GC-MS spectrum of the wastewater sample is shown in Fig. 2. The percentage frequency of detection for the wastewater compounds and their retention time are listed in Table 6. The results revealed that the primary percentage frequency, equaled 28.05%, occurred at 61.635 min and belonged to the oleic and

Table 2  
Estimation and analysis of the chosen equations

Eq. No.	Equation index	Parameters	References
1	$J_w = \frac{V}{A \times t}$	$J_w$ : water flux (L/m <sup>2</sup> ·h) $V$ : volume of the permeate water (L) $A$ : effective area of the membrane (m <sup>2</sup> ) $t$ : time of accumulation (h)	[24]
2	$R = \frac{C_f - C_p}{C_f} \times 100\%$	$C_p$ : salts concentration in permeate water (mg/L) $C_f$ : salts concentration in feedwater (mg/L)	[25]
3	$r = \frac{V_p}{V_f} \times 100\%$	$V_p$ : the permeate water volume (L) $V_f$ : feedwater volume (L)	[12]
4	Removal = $\frac{C_i - C_f}{C_i} \times 100\%$	$C_i$ : initial concentration of pollutant (mg/L) $C_f$ : final concentration of pollutant (mg/L)	[4]

Table 3  
Summary of the pretreatment type in the performed runs

Run's No.	Type of pretreatment
1	5 µm filter pretreatment
2	1 µm filter pretreatment
3	1 µm filter + ultrafilter pretreatment
4	1 µm filter pretreatment + backwashing

Table 4  
COD and TDS results of the performed runs

Item	COD (mg/L)	TDS (mg/L)
Real WW sample (before treatment)	136	763
After 5 µm filter	120	655
After 5 µm filter + RO (run 1)	24	27.9
After 1 µm filter	56	566
After 1 µm filter + RO (run 2)	20	13.53
After 1 µm filter + ultrafilter	48	456
After 1 µm filter + ultrafilter + RO (run 3)	12	10.37
After 1 µm filter + Backwash + RO (run 4)	21	12.31

NEQS for COD and TDS were 150 and 350 mg/L, respectively.

9-octadecenoic acids. Moreover, it showed a peak equaled 18.53% near 61.429 min, which referred to 9,12-octadecadienoic acid (Z,Z)-, methyl ester and linoelaidic acids, whereas the peak near 61.755 min equalled 13.55%, which referred to oleic and 6-octadecenoic acids. Other contaminants that present in the spectrum were *n*-hexadecanoic and myristic acids (12.32%); 2-(dimethylamino)ethyl methacrylate, carbonic acid, and 2-dimethylaminoethyl isobutyl ester acids (7.14%); 1-heptadecanecarboxylic acid (6.95%); 9,15-octadecadienoic acid (Z,Z)-, methyl ester (3.42%); 9,12-octadecadienoic acid (Z,Z)-, methyl ester (3.32%); 2,3,7-trimethyloctanal (3.31%); cyclopropanoic acid (2.64%); oleic, and cis-vaccenic acids (0.79%). Overall, the GC-MS analysis results illustrated

Table 5  
Heavy metals and oil content analysis of the treated wastewater [22]

Parameter	Value (mg/L)	NEQS (mg/L)	Removal (%)
Oil	0.1	10	99.5
Zn <sup>2+</sup>	0.06	1	93.8
Cu <sup>2+</sup>	0.05	1	94.1
Cr <sup>3+</sup>	0.01	1	99.5
Fe <sup>3+</sup>	0.02	1	98

that the main contaminants within the power plant wastewater sample were oleic acid, octadecenoic acid, and octadecadienoic acid (Z,Z)-, methyl ester.

### 3.2. RO membrane performance results

Several runs were performed to investigate the RO membrane performance in the desalination of the wastewater sample. Fig. 3 shows the evolution of the permeate flux with the time for runs 1, 2, 3, and 4. The permeate water of run 2 was further treated with an ultrafiltration process, and then it was used to conduct run 3. Furthermore, the RO membrane of run 2 was backwashed with deionized water, then used to perform run 4. Overall, the permeate flux of all runs dropped with the run time, and the values of the permeate flux were significantly different. For instance, run 1, which was conducted with the higher COD and TDS (120 and 655 mg/L) showed the lowest permeate flux which ranged from 19.93 to 8.4 L/m<sup>2</sup>·h, while the range of permeate flux in run 2, which was conducted with a COD and TDS of 56 and 566 mg/L was from 40.43 to 23.29 L/m<sup>2</sup>·h. On the other hand, run 3, which was carried out with the lower COD and TDS (48 and 456 mg/L) showed the highest permeate flux among the other runs which ranged from 67.49 to 51.95 L/m<sup>2</sup>·h. As the pollutants concentration in the feed channel increased, the fouling layer thickness and pollutants concentration on the membrane surface also increased, which resulted in a decline in the permeate flux. The permeate flux decline was induced by pollutant deposition on

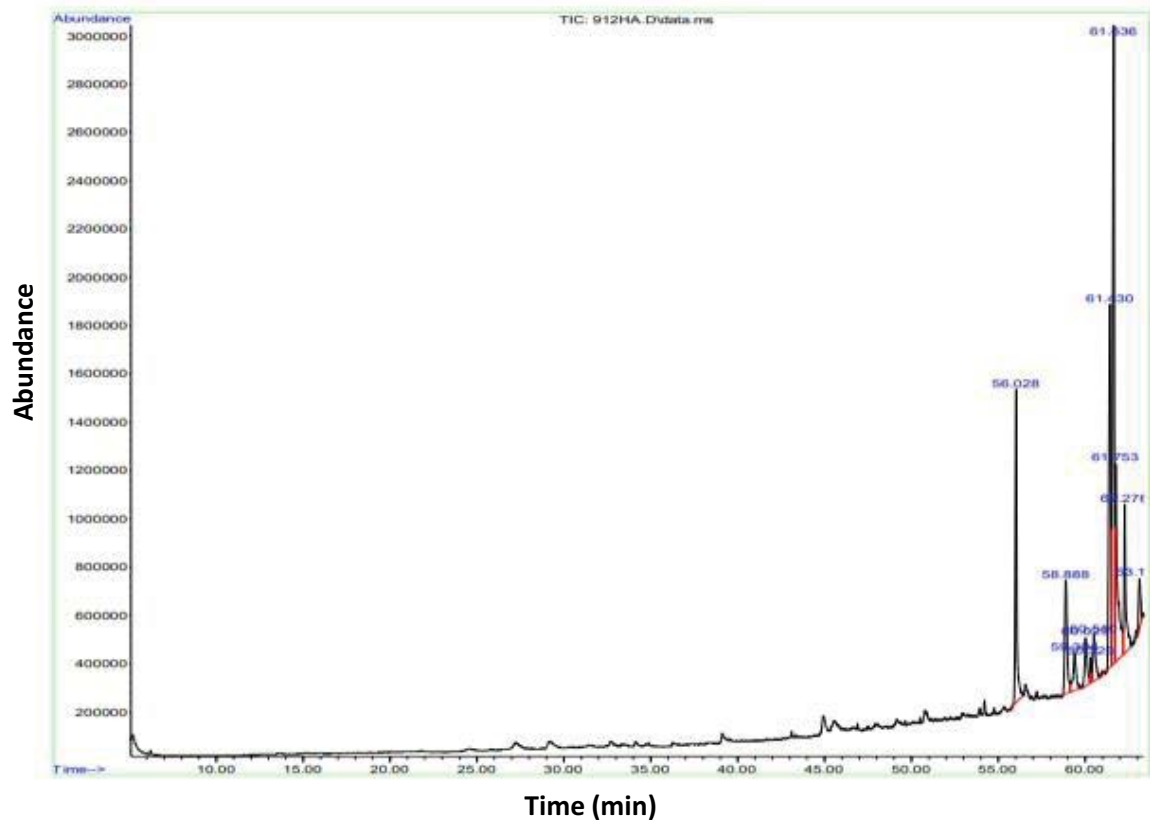


Fig. 2. GC-MS spectrum of the wastewater sample.

Table 6

Summary of wastewater compounds, peak number, retention time and percentage frequency of detection in wastewater sample

Peak No.	Compounds	Percentage frequency %	Retention time (min)
1	<i>n</i> -Hexadecanoic and myristic acids	12.32	56.028
2	2-(Dimethylamino)ethyl methacrylate, carbonic, and 2-dimethylaminoethyl isobutyl ester acids	7.14	58.886
3	2,3,7-Trimethyloctanal	3.31	59.394
4	9,12-Octadecadienoic acid (Z,Z)-, methyl ester	3.32	60.029
5	Oleic and cis-vaccenic acid	0.79	60.326
6	9,15-Octadecadienoic acid (Z,Z)-, methyl ester	3.42	60.509
7	9,12-Octadecadienoic acid (Z,Z)-, methyl ester and linoelaidic acids	18.53	61.429
8	Oleic and 9-octadecenoic acids	28.05	61.635
9	Oleic and 6-octadecenoic acids	13.55	61.755
10	1-Heptadecanecarboxylic acid	6.95	62.275
11	Cyclopropaneoctanal and 2-octyl-hexadecanoic acids	2.64	63.132

the membrane's surface, which caused a reduction in active filtration area [26]. Because all runs were conducted under identical circumstances, the variation in permeate fluxes between these runs is most likely related to differences in wastewater COD and TDS concentration.

The salt rejection percentages of the performed runs were also different, as shown in Fig. 4. Run 2 and 3 showed high salt rejection percentages compared with those of runs 1 and 4.

The low rejection of run 1 is owing to the high COD and TOC concentrations in the feedwater, which raises the salt concentration in the permeate channel due to the increased passage of salt ions across the membrane resulting in a lower salt rejection percentage. Meanwhile, the low rejection in run 4 is most likely due to the backwashed RO membrane, which was utilized in run 2. It sounds that backwashing with deionized water was inadequate to completely reactivate the membrane

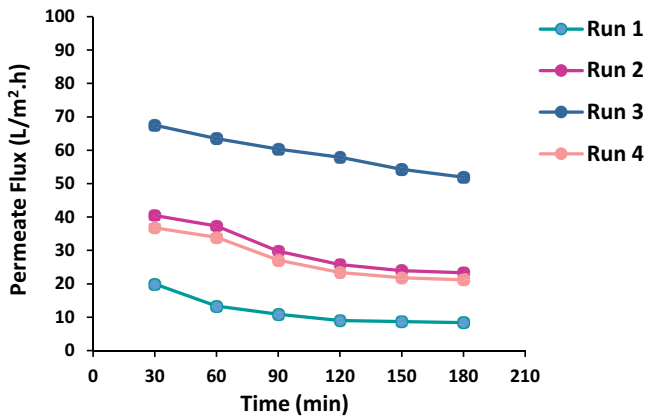


Fig. 3. Permeate fluxes of the TFC-RO membrane of the performed runs.

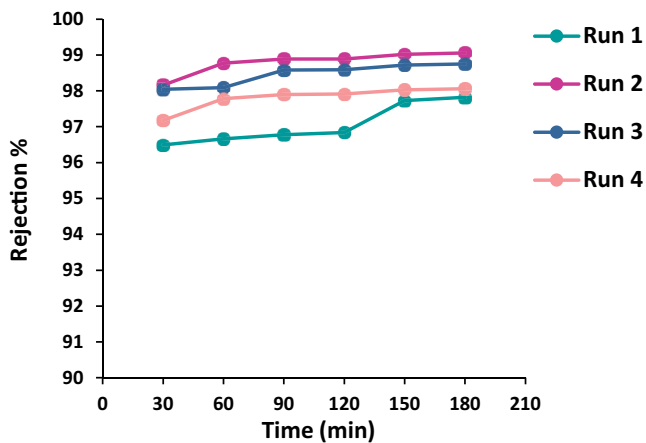


Fig. 4. Salt rejection percentages of the TFC-RO membrane of the performed runs.

since salt ions from run 2 that could not be removed by backwashing possibly remained inside the membrane pores [16].

The percentages of water recovery for runs 1, 2, 3, and 4 are shown in Fig. 5. In general, higher water recovery is related to high fluxes for all runs. For example, run 3, which had the higher permeate fluxes, showed the highest water recovery percentage (69%) compared with runs 1, 2, and 4, which showed the lowest recovery percentages (14.5%, 37.5%, and 36.25%).

Additionally, the removal percentage of COD and TDS among the performed runs (after and before the treatment) is shown in Fig. 6. Generally, the findings revealed that the tested membrane demonstrated the highest rejection level for COD and the lowest rejection level for TDS in run 1, where the membrane removed more than 80% and 95.7% of COD and TDS, respectively, as shown in Fig. 6a. However, in run 2, the membrane exhibited 64.3% and 97.6% removal of COD and TDS, respectively, as shown in Fig. 6b. Moreover, in run 3, where the UF was used as a pretreatment of the feedwater, the membrane showed a high rejection level for COD and the highest rejection levels for TDS, which were 78.6% and 98.2% of COD and TDS, respectively, as shown in Fig. 6c, which are higher than the removal

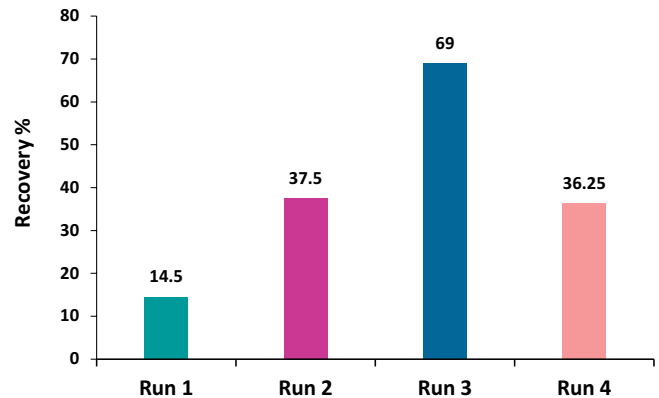


Fig. 5. Water recovery percentages of the performed runs.

percentages for COD and TDS in run 2, where the MF was utilized. In addition, in run 4, where the backwashing was performed for the membrane that was used in run 2, the membrane exhibited 62.5% and 97.8% removal of COD and TDS, respectively, as shown in Fig. 6d, which nearly equaled the removal levels of run 2 (without backwashing).

### 3.3. Membrane characterization

#### 3.3.1. Scanning electron microscope (SEM) images

Cross-sectional and surface structures of a clean TFC-PA RO membrane sample were examined via SEM analysis operating at 10 kV using several levels of magnification (1, 10, and 100 kx). The membrane sample was coated with a layer of Molybdenum (MO) before the SEM test to prevent the light from being excessively bright, which might cause poor resolution in the SEM image. As shown in Fig. 7a, the SEM image of the clean membrane revealed that the TFC-PA RO membrane had a highly rough surface structure with ridge and valley zones indicating its high porosity, which is crucial to the performance of the RO operation [27].

In addition, the cross-sectional SEM image showed that the membrane is composed of three different layers, as seen in Fig. 7b. The upper layer is the effective layer, which has a thickness of approximately 0.2  $\mu\text{m}$  [19,28]. Furthermore, the SEM image clearly revealed that the overall thickness of the TFC-PA RO membrane is around 140  $\mu\text{m}$ .

#### 3.3.2. Effect of pretreatment

The effects of utilizing a 1- $\mu\text{m}$  MF membrane and a 0.01- $\mu\text{m}$  UF membrane on the material deposited on the surface of the membrane were examined. MF is regarded as the preferred pretreatment method for the feedwater prior to the RO membrane process for removing large particulate matter [3,12]. On the other hand, UF is utilized to remove almost all colloidal particles and some of the largest dissolved pollutants from feedwater [29]. Figs. 8 and 9 show the SEM images of the fouled membranes from the pretreated wastewater using MF and UF. The SEM images demonstrate that the fouling across the membrane surface performed with the MF covers 100% of the surface (Fig. 8). In contrast,

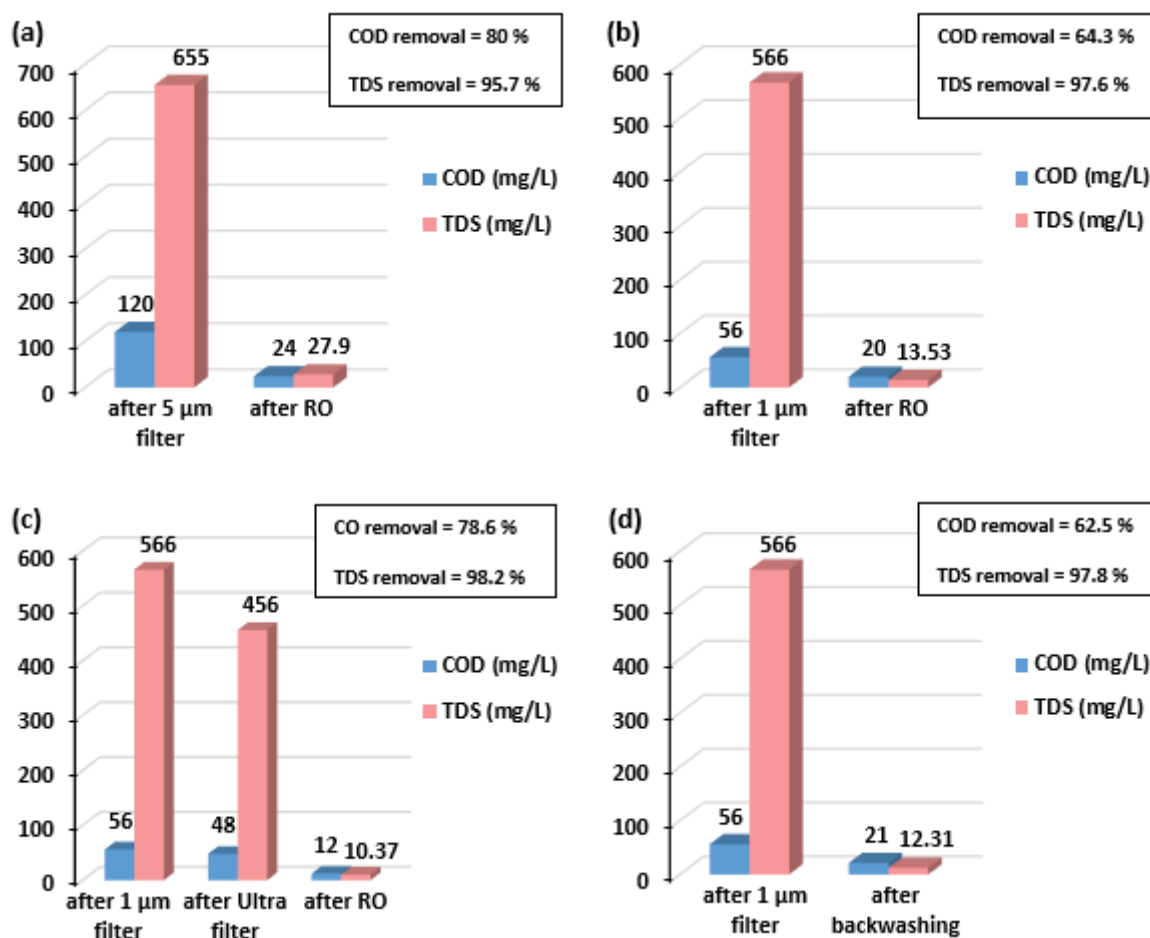


Fig. 6. Evolution of the COD and TDS concentrations for (a) run 1, (b) run 2 (MF), (c) run 3 (UF), and (d) run 4 (backwashing).

the UF fouling covers around 50% of the membrane surface (Fig. 9). This finding was supported by the fact that the initial permeate flux of the UF membrane run was greater than the initial permeate flux of the MF membrane run. For instance, the initial permeate flux in run 3, which was performed with UF, was 67.49 L/m<sup>2</sup>·h, compared to 40.43 L/m<sup>2</sup>·h in run 2, which was conducted with MF.

The results indicated that the UF membrane in run 3 captured more organics than the MF membrane in run 2. Therefore, the contaminants deposited on the membrane surface were greatly diminished, which caused a decrease in the concentration of contaminants in the permeate flux of run 3. This finding was supported by the fact that the COD removal percentage of the UF membrane run was higher than that of the MF membrane run. For example, the removal of COD in run 3 (UF) was 78.6%, compared to 64.3% in run 2 (MF).

Fig. 10 shows a comparison between cross-sectional SEM images of contaminated membranes from pretreated wastewater using MF (run 2) and UF (run 3). The SEM images showed that the membrane in run 3 contained fewer foulants than the membrane in run 2. This might be attributed to the fact that the UF membrane collected more pollutants in run 3 compared to the MF membrane in run 2.

### 3.3.3. Effect of backwashing

The performance of backwashing on the membrane reactivation was investigated. The purpose of backwashing is to control and prevent membrane fouling by removing pollutants from the surface and pores of the membrane [30]. Figs. 11 and 12 show the SEM images of the clean RO membrane and backwashed RO membrane which used in run 4. The SEM images showed that the backwashed membrane almost reverted to its original state and was nearly similar to the clean membrane. However, the initial permeate flux of run 4, conducted with backwashing, was slightly lower than that of run 2, which was performed without backwashing. For instance, the initial flux of run 4 was 36.79 L/m<sup>2</sup>·h, compared to 40.43 L/m<sup>2</sup>·h in run 2.

The results demonstrated that more foulants were removed by the backwashing process. Therefore, the pollutants deposited on the membrane surface were significantly decreased, as shown in Fig. 12 (membrane surface after backwashing) compared to Fig. 8 (membrane surface before backwashing). The concentration of contaminants in the permeate was also greatly decreased from 56 to 21 mg/L for COD and from 566 to 12.31 mg/L for TDS [Fig. 6d]. This conclusion was confirmed by the fact that the COD and TDS removal percentages of the backwashing run were

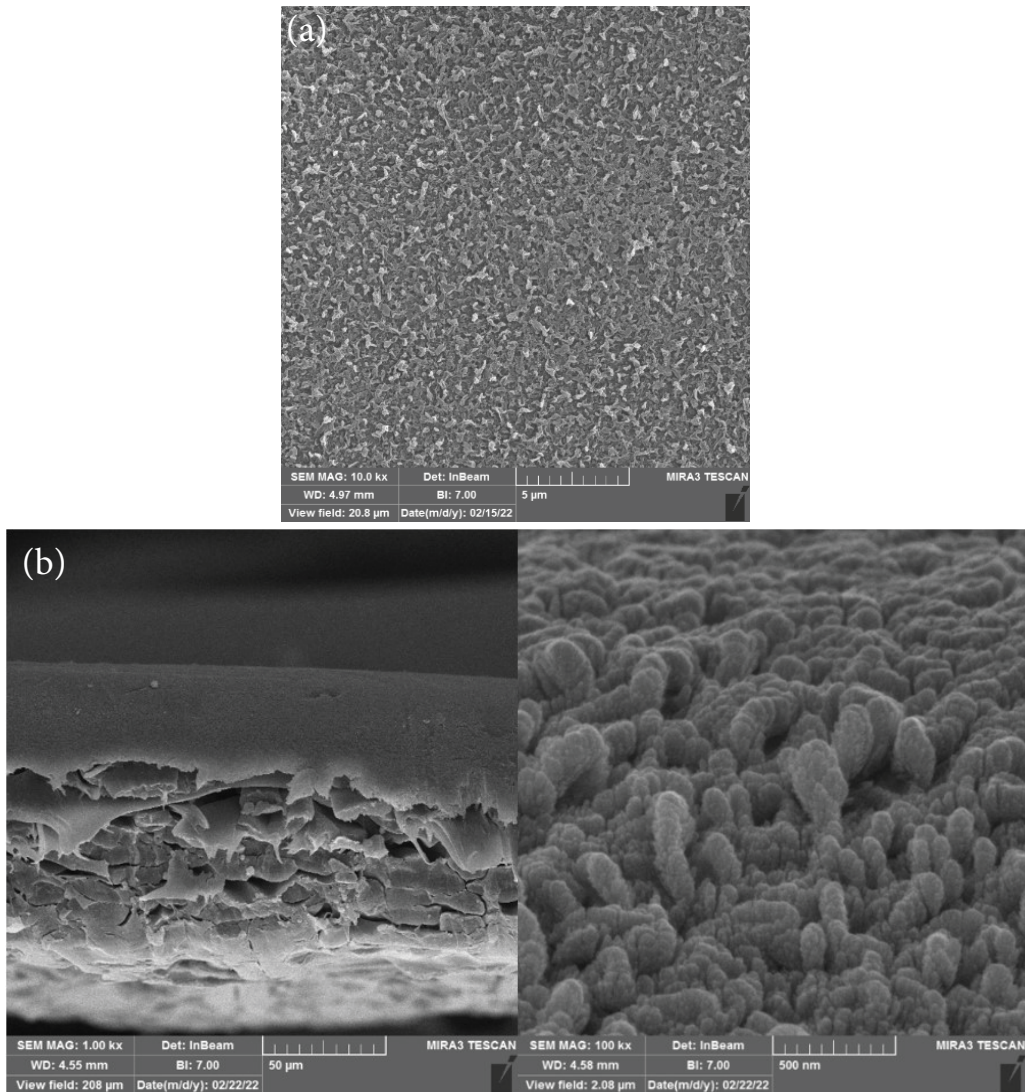


Fig. 7. SEM image of the (a) surface of clean TFC-PA RO membrane and (b) cross-section of clean TFC-PA RO membrane.

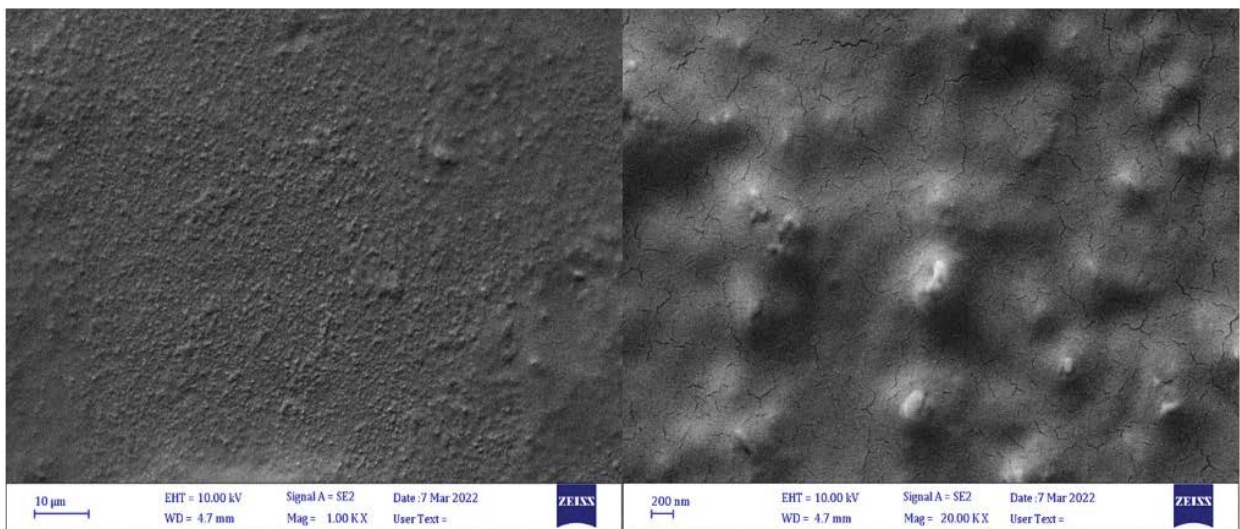


Fig. 8. SEM images of the fouled membrane for run 2 (MF pretreatment).

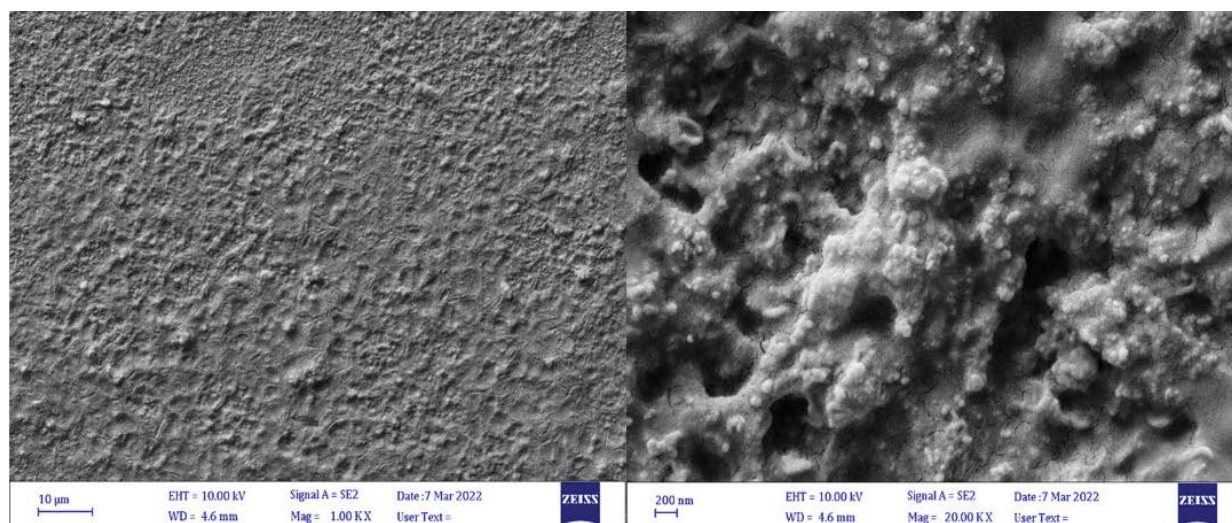


Fig. 9. SEM images of the polluted membrane for run 3 (UF pretreatment).

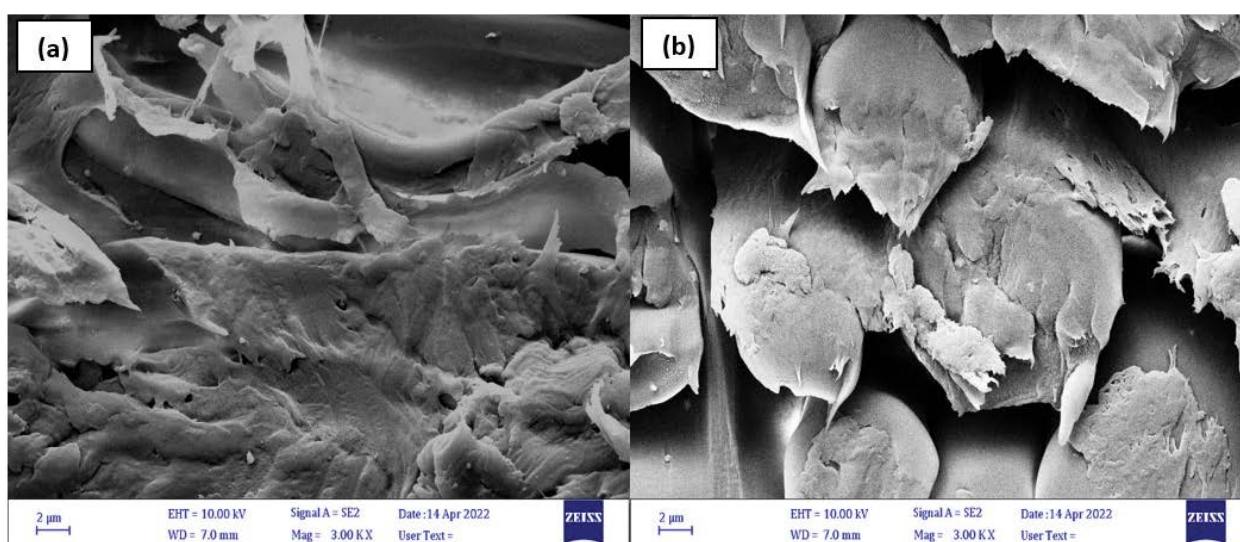


Fig. 10. SEM images of the cross-sectional of the fouled membranes from the pretreated wastewater for (a) run 2 (MF) and (b) run 3 (UF).

substantially identical to those of run 2. For example, the removal levels of COD and TDS in run 4 (with backwashing) were 62.5% and 97.8%, respectively, compared to 64.3% and 97.6% removal of COD and TDS in run 2. This indicates that backwashing is effective for reactivating the RO membrane.

### 3.4. Fourier transform infrared (FTIR) spectrum

FTIR analyses of clean and fouled membranes were performed as part of this research. Fig. 13 displays the FTIR spectrum of a clean membrane. The analysis indicated that the greatest absorption occurred between 3,903.17 and 3,336.00  $\text{cm}^{-1}$ , which is related to O–H bending due to the dominance of aliphatic alcohol functional groups. It also showed a peak at 2,968.12  $\text{cm}^{-1}$ , which referred to aliphatic hydrocarbons' C–H stretching. On the other hand, the peaks

between 1,711.75 and 507.11  $\text{cm}^{-1}$  belonged to several functional groups, particularly phenols, aliphatic alcohols, and aliphatic hydrocarbons due to the O–H and C–H bending, respectively [19,31].

The FTIR spectra of the for runs 2, 3, and the backwashed membrane are shown in Fig. 14. Similar bands at 3,911; 3,431, and 3,055  $\text{cm}^{-1}$  were seen in the FTIR spectra, which corresponded to aliphatic alcohols and phenols (O–H), amines (N–H), and aromatic hydrocarbons (C–H), respectively. The R–COOH bending of the carboxylic group also contributed to absorption peaks at 2,583 and 1,711  $\text{cm}^{-1}$  in the spectra. On the other hand, the peaks at 2,104.13; 2,104.39, and 2,104.95  $\text{cm}^{-1}$  were related to the C≡C bending of aliphatic hydrocarbons (alkyne). However, the N–H bending of primary amines was responsible for the spectral peak around 1,583  $\text{cm}^{-1}$ . Additionally, aromatic ether C–O stretching, sulfate S=O stretching, secondary amine N–H stretching,

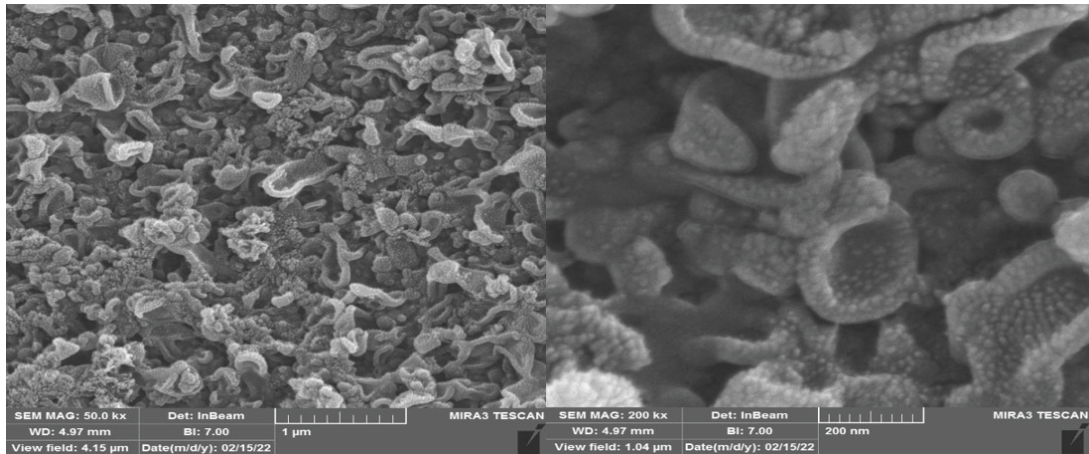


Fig. 11. SEM images of the clean membrane.

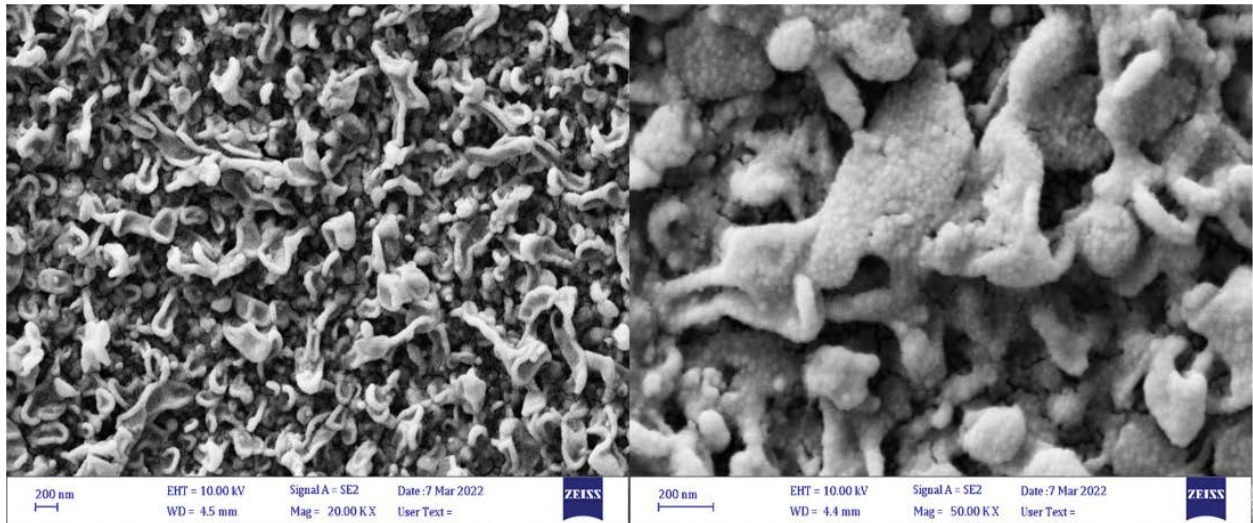


Fig. 12. SEM images of the backwashed membrane for run 4.

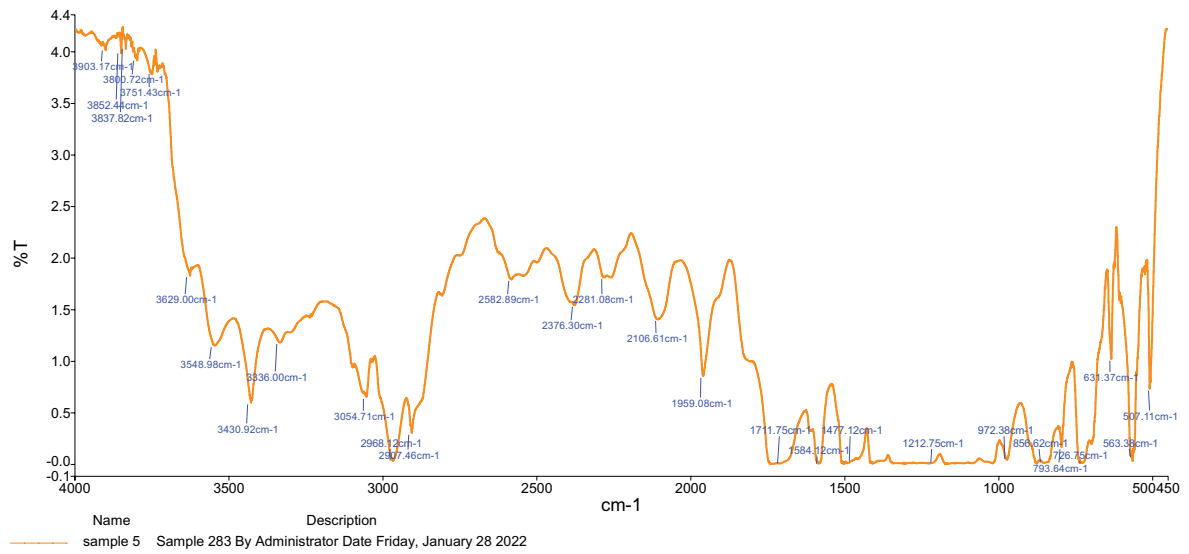


Fig. 13. FTIR spectrum of the clean TFC-PA RO membrane.

chloride C–Cl stretching, and bromide C–Br stretching contributed to the 1,275; 1,305; 1,096; 631 and 559  $\text{cm}^{-1}$  bands, respectively.

Overall, the findings showed that the majority of absorption in runs 1, 2, and the backwashed membrane was due to O–H bending of aliphatic alcohols and phenols, R–COOH bending of carboxylic acids, and C–C stretching of aliphatic hydrocarbons (alkynes) which were different from the main absorption groups found in a clean membrane's spectrum (Fig. 13), showing that there was more fouling on the membrane surface [32].

Generally, the FTIR analysis revealed that the major active groups of organic pollutants that precipitated on the surface of the membrane were aliphatic alcohols and phenols (3,600–3,200  $\text{cm}^{-1}$  and 1,150–1,100  $\text{cm}^{-1}$ ), amines (3,500–3,100  $\text{cm}^{-1}$  and 1,640–1,550  $\text{cm}^{-1}$ ), aromatic hydrocarbons (3,100–3,000  $\text{cm}^{-1}$  and 840–800  $\text{cm}^{-1}$ ), aliphatic hydrocarbons (2,990–2,850  $\text{cm}^{-1}$  and 1,300–1,200  $\text{cm}^{-1}$ ), inorganic carbonate (1,550–1,300 and 880–700  $\text{cm}^{-1}$ ), and aromatic ethers (1,300–1,200  $\text{cm}^{-1}$ ) [19].

### 3.5. Atomic force microscopy (AFM) images

In this work, the surface characteristics of the membrane were evaluated by using AFM test. The average roughness

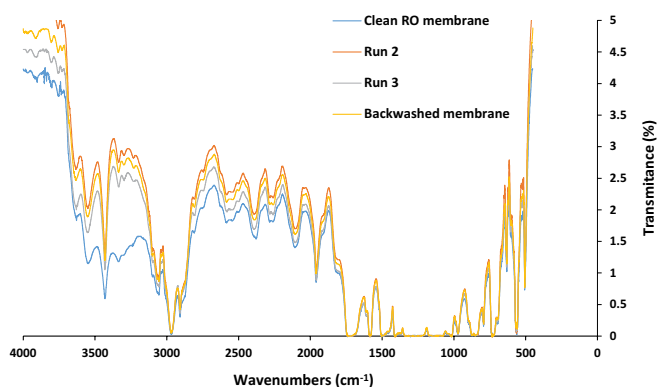


Fig. 14. FTIR spectra for the fouled TFC-PA RO membrane for (a) unused membrane, (b) run 2, (c) run 3, and (d) backwashed membrane.

of a membrane is a surface feature that influences membrane fouling owing to adsorption–desorption balance of foulants across the membrane surface [33]. Fig. 15 shows an AFM image of a clean membrane. The AFM test showed many interactions on membrane surface, indicating that the surface is rough. Although the rough surface helps prevent a variety of pollutants from passing through the membrane, but this could also enhance fouling [27]. More charged oxygen-related species are expected to be adsorbed on the surface as the surface roughness rises [34]. Moreover, the analysis revealed that the membrane was composed of numerous pores with a uniform distribution depending on their average roughness (RA), root mean square (RMS), and average diameter (AD) of 1.97, 2.99 and 17.64 nm, respectively.

Fig. 16 illustrates the AFM images of the fouled membranes for clean membrane, runs 2, 3, and backwashed membrane. In terms of average roughness (RA), root mean square (RMS), and average diameter (AD), the findings of the AFM examination of the fouled membranes among the conducted runs compared to the clean and backwashed membranes are shown in Table 7.

The AFM images illustrated that the roughness of the membrane changed among the performed runs. For example, the average surface roughness of the membrane in run

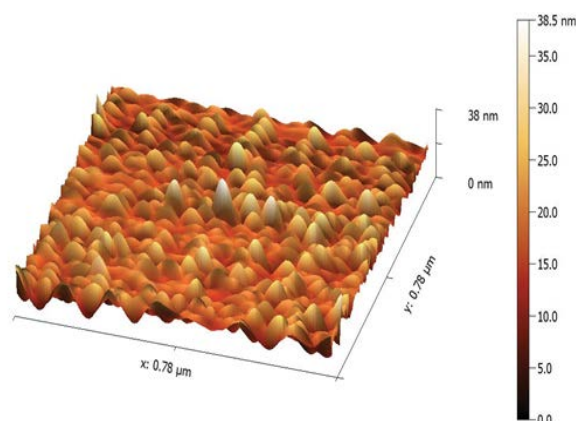


Fig. 15. AFM image of the clean RO membrane.

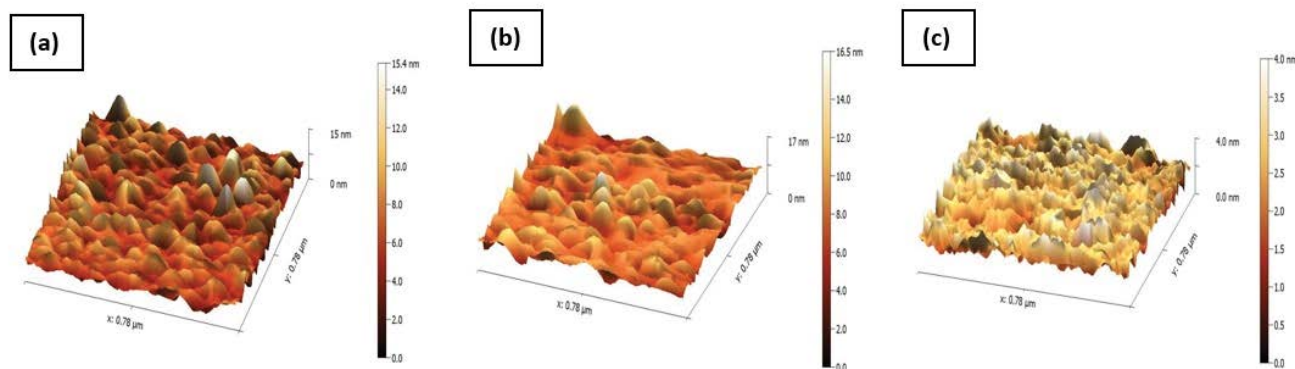


Fig. 16. AFM images of the contaminated membrane for (a) run 2, (b) run 3, and (c) backwashed membrane.

Table 7  
AFM data analysis for the fouled TFC-PA RO membranes

RO membrane	Roughness average (RA) (nm)	Root mean square (RMS) (nm)	Average diameter (AD) (nm)
Clean membrane	1.97	2.99	17.64
Run 2	1.15	1.53	8.62
Run 3	1.24	1.68	11.94
Backwashed membrane	0.41	0.57	7.02

3, which was conducted with a UF membrane, equaled 1.24 nm and was higher than that in run 2 (MF) and backwashed membrane, which equaled 1.15 and 0.41 nm, respectively. As the surface roughness increased, the membrane performance improved by increasing the filtration area and, consequently, the permeate flux [27,33]. Both RMS roughness (often regarded as more sensitive than the average roughness) and AD were also varied between the runs. The AD incensement also causes an increase in surface roughness [34]. Additionally, the analysis revealed a partial blockage of the active layer porosity of the backwashed membrane, where various foulants, including both organic and organic matter, which could not be removed by backwashing, blocked these pores, resulting in a lower rejection percentage of contaminants and a lower permeate water flux as compared to the original clean membrane.

#### 4. Conclusion

The impacts of various pretreatment methods on RO permeate flux, rejection, and recovery were examined using different filtration membranes. The majority of the RO fouling was found to be caused by particulate matter greater than 0.01  $\mu\text{m}$ . However, when MF/UF membrane filtration were applied, fouling was significantly reduced. The SEM images of the fouled RO membrane revealed that the dispersion and morphology of the precipitated pollutants on the membrane surface changed depending on the quality of the feedwater and the pretreatment type. For example, scale deposition onto the membrane surface from MF feedwater covered the entire surface of the membrane. However, the fouled material from the feedwater with UF pretreatment covered almost half of the membrane surface. SEM images of the fouled membranes demonstrated that using the UF membrane as a pretreatment lowered the extent of contaminants throughout the surface of the membranes by 50%. Therefore, the initial permeate flux of the run performed with the UF membrane was approximately 40% higher than that of the run conducted with the MF membrane. Additionally, when the UF was employed, the COD and TDS removal percentages were improved by 14% and 6%. Moreover, the AFM images showed that the roughness of the membrane changed among the performed runs. For example, the average surface roughness of the membrane in the run performed with UF (1.24 nm) was higher than that of the MF's run (1.15 nm), thus indicating the membrane performance improvement by increasing the filtration area and, consequently, the permeate flux. For backwashing performance, the SEM images of the backwashed membrane revealed that it had nearly regenerated to its

original state and was almost identical to the clean membrane in terms of appearance and contaminants removal. Despite this, the initial permeate flux of the backwashing run was around 9% lower than the original flux. Overall, the findings revealed that utilizing MF/UF as a pretreatment before the RO system considerably decreased the amounts of heavy metals and oil in the treated wastewater under the NEQS, with removal rates of 93.8%, 94.1%, 99.5%, 98%, and 99.5% for  $\text{Zn}^{2+}$ ,  $\text{Cu}^{2+}$ ,  $\text{Cr}^{3+}$ ,  $\text{Fe}^{3+}$ , and oil. Also, the water quality in terms of the COD and TDS removal was improved, which were reduced to 12 and 10.37 mg/L, respectively, generating ultrapure water and confirming that the used RO membrane technology with the UF/MF pretreatment is an effective approach to industrial wastewater treatment. Furthermore, the findings showed that backwashing was effective in reactivating the RO membrane. Therefore, it can be utilized as an alternative to chemical cleaning in order to sustain membrane longevity and functionality.

#### References

- [1] M. Kadhom, N. Albayati, H. Alalwan, M. Al-Furaiji, Removal of dyes by agricultural waste, *Sustainable Chem. Pharm.*, 16 (2020) 100259, doi: 10.1016/j.scp.2020.100259.
- [2] H.Z. Mohammed, I. Jalal, S.G. Gomes, C. Tarik, J.M.Q. Alonso, Investigation of membrane fouling in surface treatment plant using reverse osmosis process, *Mor. J. Chem.*, 4 (2016) 308–314.
- [3] T. Bakalár, H. Pavolová, L. Kozáková, P. Puškárová, M.V. Kmečová, Combined Microfiltration and Reverse Osmosis Process for Mining Water Treatment, *E3S Web Conf.*, 105 (2019) 02026, doi: 10.1051/e3sconf/201910502026.
- [4] B.A. Jasim, M.H. Al-Furaiji, A.I. Sakran, W.I. Abdullah, A competitive study using UV and ozone with  $\text{H}_2\text{O}_2$  in treatment of oily wastewater, *Baghdad Sci. J.*, 17 (2020) 1177–1182.
- [5] J. Lin, L. Ying, Z. Yufeng, L. Xundao, Study on the treatment of high salinity oil wastewater by reverse osmosis technology, *Adv. Mater. Res.*, 418–420 (2012) 90–93.
- [6] K.T. Maharaj, C.D. Hills, Water reclamation from brackish water using reverse osmosis (RO) membrane technologies in Southeast England, United Kingdom, *Inst. Water J.*, 5 (2020) 38–48.
- [7] K. Kalash, M. Kadhom, M. Al-Furaiji, Thin film nanocomposite membranes filled with MCM-41 and SBA-15 nanoparticles for brackish water desalination via reverse osmosis, *Environ. Technol. Innovation*, 20 (2020) 101101, doi: 10.1016/j.eti.2020.101101.
- [8] R.M. Garud, S.V. Kore, V.S. Kore, G.S. Kulkarni, A short review on process and applications of reverse osmosis, *Univ. J. Environ. Res. Technol.*, 3 (2011) 233–238.
- [9] L. Wang, T. Cao, J.E. Dykstra, S. Porada, P.M. Biesheuvel, M. Elimelech, Salt and water transport in reverse osmosis membranes: beyond the solution-diffusion model, *J. Environ. Sci. Technol.*, 55 (2021) 16665–16675.
- [10] M. Huajuan, A Study on Organic Fouling of Reverse Osmosis Membrane, Ph.D. Thesis, Department of Civil Engineering, National University of Singapore, 2009.

- [11] S. Salinas-Rodríguez, J. Schippers, M. Kennedy, Basic Principles of Reverse Osmosis, In: *Seawater Reverse Osmosis Desalination: Assessment and Pre-Treatment of Fouling and Scaling*, 2021, pp. 59–83.
- [12] L.F. Greenlee, D.F. Lawler, B.D. Freeman, B. Marrot, P. Moulin, Reverse osmosis desalination: water sources, technology, and today's challenges, *Water Res.*, 43 (2009) 2317–2348.
- [13] C. Balci, Understanding the operational problems and fouling characterization of RO membrane used for brackish water treatment via membrane autopsy, *Water Sci. Technol.*, 84 (2021) 3653–3662.
- [14] B.B. Van der, L. Lejon, C. Vandecasteele, Reuse, treatment, and discharge of the concentrate of pressure-driven membrane processes, *Environ. Sci. Technol.*, 37 (2003) 3733–3738.
- [15] J.Y. Park, W.W. Jeong, J.W. Nam, J.H. Kim, J.H. Kim, K. Chon, E. Lee, H.S. Kim, A. Jang, An analysis of the effects of osmotic backwashing on the seawater reverse osmosis process, *Environ. Technol.*, 35 (2014) 1455–1461.
- [16] Sh. Jiang, Y. Li, B.P. Ladewig, A review of reverse osmosis membrane fouling and control strategies, *Sci. Total Environ.*, 595 (2017) 567–583.
- [17] N.F. Zulkefli, N.H. Alias, N.S. Jamaluddin, N.F.A. Abdullah, S.F. Abdul Manaf, N.H. Othman, F. Marpani, M.S. Mat-Shayuti, T.D. Kusworo, Recent mitigation strategies on membrane fouling for oily wastewater treatment, *Membranes (Basel)*, 12 (2022), doi: 10.3390/membranes12010026.
- [18] H. Chang, H. Liang, F. Qu, B. Liu, H. Yu, X. Du, G. Li, S.A. Snyder, Hydraulic backwashing for low-pressure membranes in drinking water treatment: a review, *J. Membr. Sci.*, 540 (2017) 362–380.
- [19] D.E. Sachit, J.N. Veenstra, Foulant analysis of three RO membranes used in treating simulated brackish water of the Iraqi marshes, *Membranes (Basel)*, 7 (2017) 1–25, doi: 10.3390/membranes7020023.
- [20] I. Koyuncu, M.R. Wiesner, Morphological variations of precipitated salts on NF and RO membranes, *Environ. Eng. Sci.*, 24 (2007) 602–614.
- [21] M. Jendoubi, K. Makhlof, M. Boulabiar, H. Elfil, RO Membrane Autopsy, TJS Water, Tunisian Japon Symposium Conference, Tunis, 2018. Available at: <http://dx.doi.org/10.13140/RG.2.2.29250.02240>
- [22] NEQS (National Environmental Quality Standards) for Municipal and Liquid Industrial Effluents, Islamabad, Pakistan, Revised December 28, 1999. Available at: <https://www.elaw.org/system/files/RevisedNEQS.pdf>
- [23] D.E. Sachit, J.N. Veenstra, Analysis of reverse osmosis membrane performance during desalination of simulated brackish surface waters, *J. Membr. Sci.*, 453 (2014) 136–154.
- [24] M.H. Al-Furaiji, J.T. Arena, M. Chowdhury, N. Benes, A. Nijmeijer, J.R. McCutcheon, Use of forward osmosis in treatment of hyper-saline water, *Desal. Water Treat.*, 133 (2018) 1–9.
- [25] M. Kadhom, B. Deng, Metal-organic frameworks (MOFs) in water filtration membranes for desalination and other applications, *Appl. Mater. Today*, 11 (2018a) 219–230.
- [26] N.O. Kariem, D.E. Sachit, Z.Q. Ismael, The performance of a spiral wound RO membrane to desalinate a brackish groundwater in the middle of Iraq, *Desal. Water Treat.*, 136 (2018) 72–82.
- [27] D. Norberg, S. Hong, J. Taylor, Y. Zhao, Surface characterization and performance evaluation of commercial fouling resistant low-pressure RO membranes, *Desal. Water Treat.*, 202 (2007) 45–52.
- [28] A. Adeniyi, R.K.K. Mbaya, M.S. Onyango, A.P.I. Popoola, M.E. Sethoga, V.T. Hlongwane, J.M. Mosesane, O.I. Olukunle, J. Maree, Water recovery and rejection of organochloride pesticides during reverse osmosis process, *J. Comput. Theor. Nanosci.*, 14 (2017) 5103–5109.
- [29] M. Clever, F. Jordt, R. Knauf, N. Rübiger, M. Rüdibusch, R. Hilker-Scheibel, Process water production from river water by ultrafiltration and reverse osmosis, *Desal. Water Treat.*, 131 (2000) 325–336.
- [30] E. Akhondi, F. Wicaksana, A.G. Fane, Evaluation of fouling deposition, fouling reversibility and energy consumption of submerged hollow fiber membrane systems with periodic backwash, *J. Membr. Sci.*, 452 (2014) 319–331pp.
- [31] LBNL, Characteristic IR Band Positions, U.S. Department of Energy National Laboratory, University of California, USA, Characteristic IR Band Positions (lbl.gov), 2022.
- [32] M. Karime, S. Bouguecha, B. Hamrouni, RO membrane autopsy of Zarzis brackish water desalination plant, *Desal. Water Treat.*, 220 (2008) 258–266.
- [33] W.Kh. Al-Musawy, M.H. Al-Furaiji, Q.F. Alsally, Synthesis and characterization of PVC-TFC hollow fibers for forward osmosis application, *J. Appl. Polym. Sci.*, 138 (2021) 50871, doi: 10.1002/app.50871.
- [34] B.R. Kumar, T.S. Rao, AFM studies on surface morphology, topography and texture of nanostructured zinc aluminum oxide thin films, *Dig. J. Nanomater. Biostruct.*, 7 (2012) 1881–1889.